

FEM (Finite Element Method) Simulation of the Three-Dimensional Boundary Layer Close to a Rotating Semi-spherical Electrode in Electrochemical Cells

Rachel Manhães de Lucena

Norberto Mangiavacchi

Group of Environmental Studies for Water Reservoirs – GESAR/State University of Rio de Janeiro, Rua Fonseca Teles, 121, 20940-200, Rio de Janeiro, RJ, Brazil

rachel.lucena@gmail.com, norberto.mangiavacchi@gmail.com

Gustavo R. Anjos

Massachusetts Institute of Technology, 77 Massachusetts Avenue Room NW12-306 MA 02139-4301, Cambridge, USA

gustavo.rabello@gmail.com

José Pontes

Metallurgy and Materials Engineering Department – Federal University of Rio de Janeiro, PO Box 68505, 21941-972 Rio de Janeiro, RJ, Brazil

jopontes@metalmat.ufrj.br

Abstract. Iron rotating disk electrodes are widely in applied electrochemistry due to the fact of requiring an easily built experimental setup and to the existence of a simple semi-analytical similarity solution for the steady hydrodynamic equations describing the flow close to the electrode. Based on this solution the current in the cell is theoretically evaluated and compared to the experimental results. A caveat of such experimental apparatus results from the fact that, particularly at high current regimes, dissolution of the iron electrode in the 1 M H_2SO_4 solution of the electrolyte endangers the geometry of the electrode surface and the electrode no longer can be used. An alternative to overcome the problem consists in using rotating semi-spherical electrodes, which keep the geometry in the dissolution process. However, no similarity solution exists for the complete hydrodynamic equations exits for this case. First, a boundary layer approximation is required to describe the flow in the neighborhood of the electrode and second, a solution is found, in terms of a power series of the polar angle, multiplying functions describing the dependency of the velocity components on the radial coordinate. In this work we briefly review the principles of the power series solution for the steady solution of the boundary layer developed by constant viscosity electrolytes close to rotating semi-spherical electrodes and propose a numerical Finite Element (FEM) procedure to obtain the velocity profiles for polar angles θ (southern direction) ranging $0 \leq \theta \leq \pi/2$. Spatial discretization of the diffusive and pressure terms is performed by the Galerkin method, and of the material derivative, through the Semi-lagrangian method. The numerical code, developed in C++, uncouples the velocity and pressure through the discrete projection method. Conjugate gradient method is used to solve the velocity whereas pressure is solved with the generalized minimal residual method (GMRES). The results obtained are compared with the semi-analytical solution obtained by the power series method. The effect of boundary conditions imposed in the simulations at the equator plane is analyzed and compared to the conditions assumed in the semi-analytical solution.

Keywords: corrosion, rotating disk flow, semi-spherical electrode, finite element method, boundary layer

1. INTRODUCTION

The hydrodynamic field developed close to the axis of a large rotating disk belongs to the restricted class of problems admitting a analytical or semi-analytical similarity solution of the hydrodynamic equations von Kármán (1921). The angular velocity imposed to the fluid at the surface gives rise to a centrifugal effect and to a radial flow outwards. Continuity requires that the flow be replaced by an incoming one that approaches the disk. Close to the surface, the axial velocity of the incoming flow is reduced and the centrifugal effect appears. Among the applications of von Kármán's rotating disk flow we mention aerodynamics, flow in turbomachineries, crystal growth, heat transfer in electronic equipments, surgical devices circulatory assistance.

von Kármán's flow find an important application in applied electrochemistry, where cells using iron rotating disk electrodes are widely used due to the fact of requiring an easily built experimental setup and to the existence of von Kármán's solution. Based on this solution the current in the cell is theoretically evaluated and compared to the experimental results. A caveat of such experimental apparatus results from the fact that, particularly at high current regimes, dissolution of the iron electrode in the 1 M H_2SO_4 solution of the electrolyte endangers the geometry of the electrode surface and the electrode no longer can be used. An alternative to overcome the problem consists in using rotating semi-spherical electrodes, which keep the geometry in the dissolution process. However, no similarity solution exists for the complete

hydrodynamic equations exists for this case. First, a boundary layer approximation is required for the equations governing the flow in the neighborhood of the electrode and second, a solution is found, in terms of a power series of the polar angle, multiplying functions describing the dependency of the velocity components on the radial coordinate.

Setups with both rotating disk and rotating semi-spherical electrodes have been used by the group of Applied Electrochemistry of the Federal University of Rio de Janeiro (PEMM/COPPE/UFRJ). The experimental setup features cylindrical beaker containing the electrolyte, a counter-electrode consisting of a platinum mesh disposed along the cell sidewalls, a reference electrode and rotating disk or semi-spherical working electrode. The working electrode consists of a 5mm diameter iron electrode laterally lined with a resin, resulting in a cylindrical rod with 10mm diameter. The current flow through the 5mm diameter lower surface of the rod. A rotating semi-spherical electrode cell is schematically shown in Fig. 1.

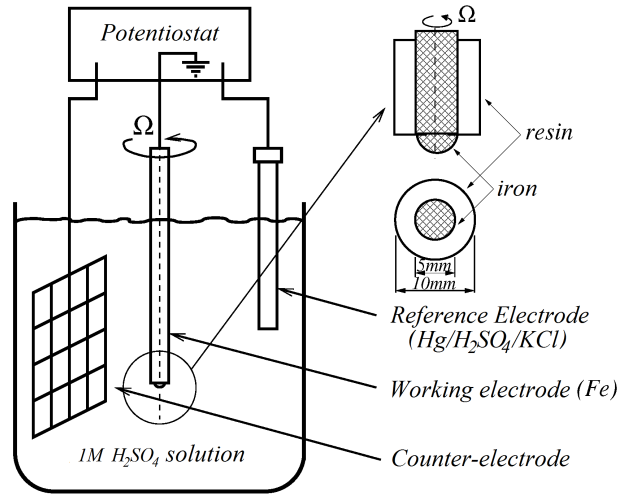


Figure 1. Electrochemical cell with a rotating semi-spherical electrode

The flow close to a rotating semi-sphere, or rotating semi-sphere electrode was studied by Lamb (1932), Bickley (1938), Howarth (1951), Godinez (1996) and Barcia *et al.* (1998). Godinez (1996) addressed the steady flow close to a rotating semi-spherical electrode by obtaining a solution in the form of an expansion for the velocity components, in terms of a power series of the polar angle. This solution satisfies the boundary layer equations for the flow close to a rotating semi-sphere. The steady boundary layer equations were also solved by a finite differences scheme.

In this work we briefly review the principles of the power series solution for the steady solution of the boundary layer developed by constant viscosity electrolytes close to rotating semi-spherical electrodes and propose a numerical Finite Element (FEM) procedure to obtain the velocity profiles for polar angles θ (southern direction) ranging $0 \leq \theta \leq \pi/2$. The results are compared to the ones obtained by Godinez, as a step towards validating the code. We used as a method to solve the finite element method (FEM) and validate the results by comparison with Godinez's results.

2. METHODOLOGY

2.1 Power Series Method

This method consists in finding solution in terms of a power series of the variables describing the system state and obeying an equation or a system of differential equations.

Equations governing Godinez (1996) the flow close to a rotating sphere are the continuity and momentum equations of the velocity components along the radial and polar directions (r, θ, ϕ).

The hydrodynamic boundary layer equations, applicable to the flow close to a rotating semi-sphere obtained under the assumption of high Reynolds numbers are given by:

$$\frac{\partial v_r}{\partial r} + \frac{1}{r_0} \frac{\partial v_\theta}{\partial \theta} + \frac{\cot \theta}{r_0} v_\theta = 0 \quad (1)$$

$$v_r \frac{\partial v_\theta}{\partial r} + \frac{v_\theta}{r_0} \frac{\partial v_\theta}{\partial \theta} - \frac{\cot \theta}{r_0} v_\phi^2 = \nu \frac{\partial^2 v_\theta}{\partial r^2} \quad (2)$$

$$v_r \frac{\partial v_\phi}{\partial r} + \frac{v_\theta}{r_0} \frac{\partial v_\phi}{\partial \theta} + \frac{\cot \theta}{r_0} v_\theta v_\phi = \nu \frac{\partial^2 v_\phi}{\partial r^2}. \quad (3)$$

In the above equations, r_0 is the radius of the semi-sphere and ν , the kinematic viscosity of the fluid. Boundary conditions for Eqs. (1)-(3) are, in $r = r_0$: $v_r = v_\theta = 0$ and $v_\phi = r_0 \bar{\Omega} \sin \theta$, where $\bar{\Omega}$ is the steady angular velocity imposed to the

electrode.

Upon assuming symmetry along the azimuthal direction ϕ , we express the velocity components in terms of the polar angle and the nondimensional radial coordinate η given by:

$$v_\theta = r_0 \bar{\Omega} F(\theta, \eta), \quad v_\phi = r_0 \bar{\Omega} G(\theta, \eta), \quad v_r = (\nu_\infty \bar{\Omega})^{1/2} H(\theta, \eta) \quad \text{and} \quad \eta = (\bar{\Omega}/\nu)^{1/2} (r - r_0). \quad (4)$$

The nondimensional equivalent equations in directions η and θ , respectively, radial and meridional directions of a semi-spherical, are:

$$\frac{\partial H}{\partial \eta} + \frac{\partial F}{\partial \theta} + \cot \theta F = 0 \quad (5)$$

$$H \frac{\partial F}{\partial \eta} + F \frac{\partial F}{\partial \theta} - \cot \theta G^2 = \nu \frac{\partial^2 F}{\partial \eta^2} = 0 \quad (6)$$

$$H \frac{\partial G}{\partial \eta} + F \frac{\partial G}{\partial \theta} + \cot \theta FG = \nu \frac{\partial^2 G}{\partial \eta^2} = 0. \quad (7)$$

The power series method was applied to the system of Eqs. (5)-(7) where the nondimensional functions are given by:

$$F(\theta, \eta) = \sum_{i=1}^n \theta^{2i-1} F_{2i-1}(\eta), \quad G(\theta, \eta) = \sum_{i=1}^n \theta^{2i-1} G_{2i-1}(\eta), \quad H(\theta, \eta) = \sum_{i=1}^n \theta^{2i-2} H_{2i-1}(\eta) \quad \text{and}$$

$$\cot \theta = \frac{1}{\theta} - \frac{\theta}{3} - \frac{\theta^3}{45} - \frac{2\theta^5}{945} - \dots$$

We restrict the number of terms of the series expansion of functions F, G, H and $\cot \theta$ to $n = 10$, obtaining thus ten systems of differential equations, numerically solved by Newton's method.

2.2 Finite Element Method

The Finite Element method is a numerical technique of approximations (and discretizations). It is a important tool to solve problems that involve partial differential equations. The domain of problem is subdivided in sub-domains named finite elements, and over this elements are applied functions of interpolation that approximate to solution this sub-domain, the set of sub-domain's solutions is the approximate solution of the problem.

2.2.1 Governing Equations and Variational Formulation

The equations that model the incompressible flow of a newtonian fluid with constant viscosity and determine the hydrodynamic field nondimensional form are given by:

$$\frac{D\mathbf{v}}{Dt} = -\frac{1}{\rho} \nabla p + \frac{1}{Re} \nabla \cdot [\nu (\nabla \mathbf{v} + \nabla \mathbf{v}^T)] \quad \text{and} \quad (8)$$

$$\nabla \cdot \mathbf{v} = 0, \quad (9)$$

where $\mathbf{v}(\mathbf{x}, t)$ is velocity vector, $p(\mathbf{x}, t)$ is the pressure, ρ is the specific mass of the fluid, ν is the kinematic viscosity of the fluid and Re is the Reynolds number. Equation (8) is the Navier-Stokes equation and Eq. (9) is the continuity equation.

Boundary conditions to the Eqs (8) and (9) are $\mathbf{v} = \mathbf{v}_\Gamma$ on Γ_1 , $\mathbf{v}_t = 0$ and $\sigma^{nn} = 0$ on Γ_2 , respectively to velocity and pressure.

The variational formulation is obtained by properly weighting the Navier-Stokes equations and continuity equation. We obtain:

$$\int_{\Omega} \frac{D\mathbf{v}}{Dt} \cdot \mathbf{w} \, d\Omega - \frac{1}{\rho} \int_{\Omega} p [\nabla \cdot \mathbf{w}] \, d\Omega + \frac{1}{Re} \int_{\Omega} [(\nabla \mathbf{v} + \nabla \mathbf{v}^T)] : \nabla \mathbf{w}^T \, d\Omega = 0 \quad (10)$$

$$\int_{\Omega} [\nabla \cdot \mathbf{v}] q \, d\Omega = 0. \quad (11)$$

where functions \mathbf{w} and q are *weighting functions* defined in the space $\mathcal{V} := \{\mathbf{w} \in \mathcal{H}^1(\Omega) \mid \mathbf{w} = 0 \text{ in } \Gamma_c\}$, where \mathbf{u}_c is the essential boundary condition value, Γ_c a possible boundary for the domain Ω , $\mathcal{H}^1(\Omega) := \left\{ \mathbf{u} \in \mathcal{L}^2(\Omega) \mid \frac{\partial \mathbf{u}}{\partial x_i} \in \mathcal{L}^2(\Omega), i = 1, \dots, n \right\}$ and $\mathcal{L}^2(\Omega)$ is the *Lebesgue space*, i. e., the space of all *square integrable* functions.

2.2.2 Semi-discrete Galerkin method

The semi-discrete Galerkin Method provides a partial discretization where the functions that approximate a solution for the governing equations (Eqs.(10) and (11)) comprise a linear combination of shape functions depending on the time of

functions intended to depend on the space coordinates. Following this procedure we denote by NV and NP the number of velocity, pressure and concentration nodes, respectively, of the discrete grid of elements of the original domain Ω . The following semi-discrete approximation functions are obtained:

$$\begin{aligned} v_x(\mathbf{x}, t) &\approx \sum_{i=1}^{NV} u_i(t) N_i(\mathbf{x}), & v_y(\mathbf{x}, t) &\approx \sum_{i=1}^{NV} v_i(t) N_i(\mathbf{x}), & v_z(\mathbf{x}, t) &\approx \sum_{i=1}^{NV} w_i(t) N_i(\mathbf{x}) \quad \text{and} \\ p(\mathbf{x}, t) &\approx \sum_{i=1}^{NP} p_i(t) P_i(\mathbf{x}), \end{aligned}$$

where the coefficients u_i, v_i, w_i and p_i denote continuous functions in the time (t) and functions $N_i(\mathbf{x})$ and $P_i(\mathbf{x})$ are interpolation functions at specified positions \mathbf{x} for the velocity and pressure, respectively.

The discretized system becomes, in matrix form:

$$\begin{aligned} \mathbf{M}\dot{\mathbf{v}} + \frac{1}{Re}\mathbf{K}\mathbf{v} - \mathbf{G}\mathbf{p} &= 0 \\ \mathbf{D}\mathbf{v} &= 0, \end{aligned}$$

where

$$\begin{aligned} \mathbf{M} &= \begin{bmatrix} \mathbf{M}_x & 0 & 0 \\ 0 & \mathbf{M}_y & 0 \\ 0 & 0 & \mathbf{M}_z \end{bmatrix}, & \mathbf{K} &= \begin{bmatrix} \mathbf{K}_x & \mathbf{K}_{xy} & \mathbf{K}_{xz} \\ \mathbf{K}_{yx} & \mathbf{K}_y & \mathbf{K}_{yz} \\ \mathbf{K}_{zx} & \mathbf{K}_{zy} & \mathbf{K}_z \end{bmatrix}, & \mathbf{G} &= [\mathbf{G}_x \quad \mathbf{G}_y \quad \mathbf{G}_z]^T, \\ \mathbf{K}_x &= 2\mathbf{K}_{xx} + \mathbf{K}_{yy} + \mathbf{K}_{zz}, & \mathbf{K}_y &= \mathbf{K}_{xx} + 2\mathbf{K}_{yy} + \mathbf{K}_{zz}, & \mathbf{K}_z &= \mathbf{K}_{xx} + \mathbf{K}_{yy} + 2\mathbf{K}_{zz}, \\ \mathbf{D} &= [\mathbf{D}_x \quad \mathbf{D}_y \quad \mathbf{D}_z], & \dot{\mathbf{v}} &= [\dot{\mathbf{u}} \quad \dot{\mathbf{v}} \quad \dot{\mathbf{w}}]^T & \text{and } \mathbf{v} &= [\mathbf{u} \quad \mathbf{v} \quad \mathbf{w}]^T. \end{aligned}$$

2.2.3 Semi-lagrangian method

The semi-lagrangian method has been widely used since the 80's in the solution of convective problems. The main favorable features are stability and the large time steps allowed.

One can observe the use of a discrete representation of the substantial derivative in the discretized weak form of the governing equations. In this section we apply the semi-lagrangian method to the substantial derivatives of the governing equations. We obtain:

$$\frac{D\mathbf{v}}{Dt} = \frac{\mathbf{v}_i^{n+1} - \mathbf{v}_d^n}{\Delta t} \quad (12)$$

The global matrix system takes the following discrete form:

$$\mathbf{M} \left(\frac{\mathbf{v}_i^{n+1} - \mathbf{v}_d^n}{\Delta t} \right) + \frac{1}{Re}\mathbf{K}\mathbf{v}^{n+1} - \mathbf{G}\mathbf{p}^{n+1} = 0 \quad (13)$$

$$\mathbf{D}\mathbf{v}^{n+1} = 0, \quad (14)$$

where $\mathbf{v}_d^n = \mathbf{v}^n(x_d, t^n)$ and x_d refers to the starting point in the time $t^n \leq t \leq t^{n+1}$ with initial condition $x(t^{n+1}) = x_i$.

2.2.4 Elements of the mesh

The element implemented to calculate of the velocities from Navier-Stokes equations was a tetradic element namely by *MINI element*, this element has one more degree of freedom located in the centroid of the tetrahedron. The polynomial of interpolation is of third degree for this element because the element is a tetrahedron.

2.2.5 Discrete projection method

The discrete projection method based in the LU decomposition is obtained of block decomposition of linear system resulting. The decoupling of velocity and pressure is made after the discretization in the position and in the time of the governing equations.

The Eqs. (13) and (14) form a equations system that can be represented by:

$$\begin{bmatrix} B & -\Delta t G \\ D & 0 \end{bmatrix} \cdot \begin{bmatrix} \mathbf{v}^{n+1} \\ p^{n+1} \end{bmatrix} = \begin{bmatrix} r^n \\ 0 \end{bmatrix} + \begin{bmatrix} bc_1 \\ bc_2 \end{bmatrix} \quad (15)$$

where $\mathbf{v}^{n+1} = [u_1^{n+1}, \dots, u_{Nu}^{n+1}, v_1^{n+1}, \dots, v_{Nv}^{n+1}, w_1^{n+1}, \dots, w_{Nw}^{n+1}]^T$, $p^{n+1} = [p_1^{n+1}, \dots, p_{Np}^{n+1}]^T$, Nu, Nv, Nw and Np are the unknowns number for velocity in the directions x, y and z and pressure, respectively.

The matrix B is given by:

$$B = M + \frac{\Delta t}{Re} K, \quad (16)$$

the r^n is given by:

$$r^n = -\Delta t(M\mathbf{v}_d^n) + M\mathbf{v}^n \quad (17)$$

and bc_1 and bc_2 are the boundary conditions.

Using the canonical LU factorization by blocks on the system (15), we obtain:

$$\begin{bmatrix} B & 0 \\ D & \Delta t DB^{-1}G \end{bmatrix} \cdot \begin{bmatrix} I & -\Delta t B^{-1}G \\ 0 & I \end{bmatrix} \cdot \begin{bmatrix} \mathbf{v}^{n+1} \\ p^{n+1} \end{bmatrix} = \begin{bmatrix} r^n \\ 0 \end{bmatrix} + \begin{bmatrix} bc_1 \\ bc_2 \end{bmatrix} \quad (18)$$

As we have B^{-1} the system (18) gives rise to the *Uzawa* method (Chang *et al.*, 2002) which uses exact factorization. But its solution is very expensive computing cost due the fact the inversion of B each iteration. Alternatively we use the approximate factorization which approximates the matrix B^{-1} for B_L^{-1} , where B_L is the *lumped* matrix. The *lumping* technique consists of adding all the attributions of a line and locate them in the main diagonal.

3. RESULTS

In this section we presented the results about this work. We consider the domain of the semi-sphere how $R = r_0 + dr$, where r_0 is the physical radius of the semi-sphere and dr is the thickness of the mesh. We used the follows dimensions: $R = 55$, i.e., $r_0 = 40$ and $dr = 15$.

3.1 Computational mesh for a rotating semi-spherical electrode

The computational mesh used in the FEM's simulations is shown in the Fig. 2, this mesh mimics the geometry semi-spherical of the electrode for the three-dimensional numerical simulations.

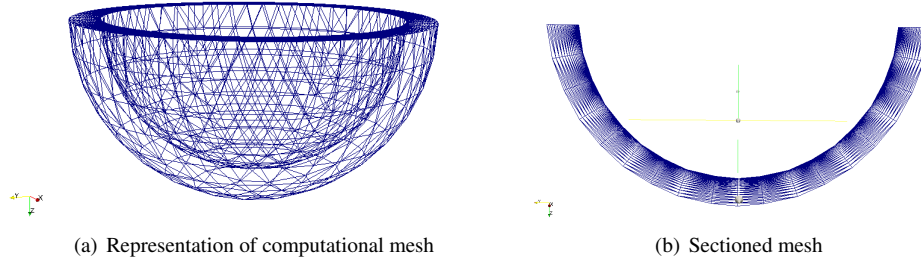


Figure 2. Computational mesh

3.2 Boundary conditions

Figure 3 helps us how the boundary conditions were applied. In the Fig. 3 the solid surface A were applied $v_z = 0$, $v_x = -\Omega y$ and $v_y = \Omega x$. In the side B we applied Neumann's condition at velocity ($\mathbf{n} \cdot \nabla \mathbf{v} = 0$) and Dirichlet's condition for the pressure ($p = 0$). And the sides C and D were applied the pressure equal to zero.

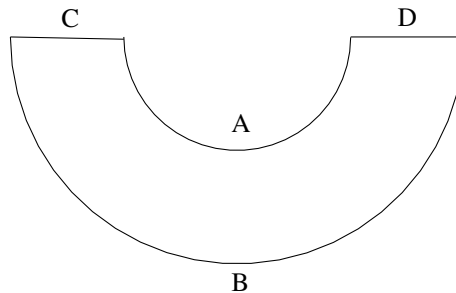


Figure 3. Representation of boundary conditions of semi-spherical electrode

3.3 Qualitative results

In this section we present the behavior of the fluid, we show the flow close to a rotating semi-spherical electrode. Figures 4, 5 and 6 show that the velocity field are correct and from angles θ superior of 60° the solutions present one recirculation due the fact we was applied pressure equal to zero at to the equator.

We can also observe to the development of the boundary layer from the pole of the semi-sphere to the equator.

Velocity magnitude

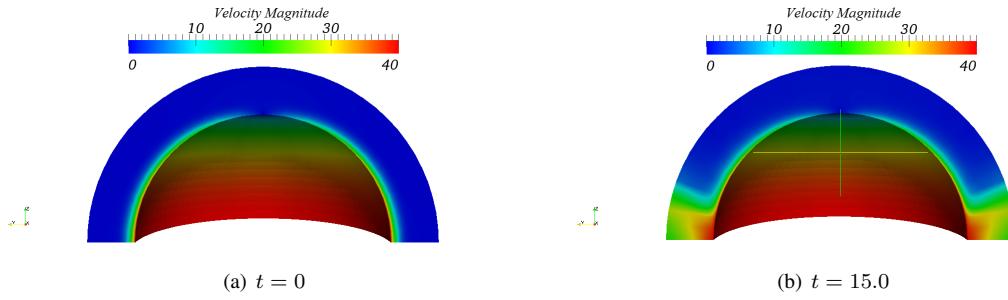


Figure 4. Velocity magnitude at two times

The z component of the velocity

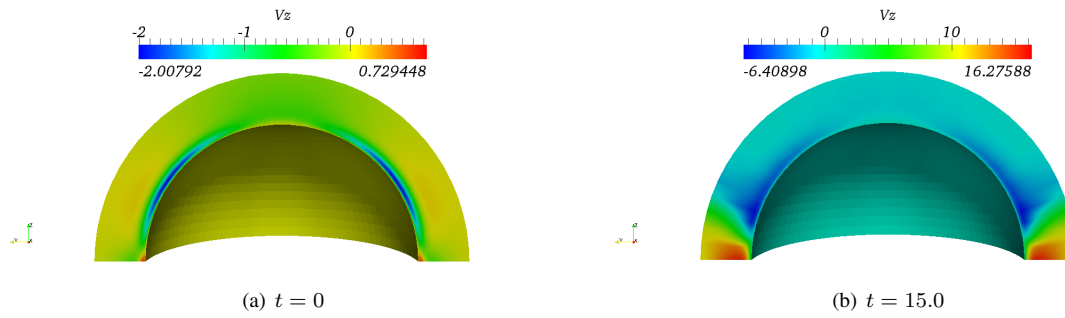


Figure 5. z component of the velocity at two times

The x component of the velocity

The behavior of the flow in the directions x and y are symmetric, thus we show just at the direction x .

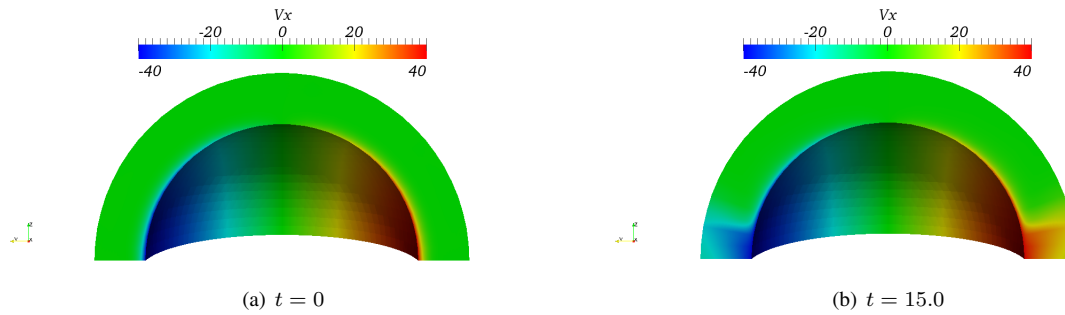


Figure 6. x component of the velocity at two times

3.4 Quantitative results

Figure 7 shows the numerical results obtained by FEM's simulations compared with the semi-analytical results obtained by Godinez (1996). We present the velocity profiles for angles $\theta = 20^\circ$, $\theta = 40^\circ$, $\theta = 60^\circ$ and $\theta = 80^\circ$.

The Fig. 7 confirms that has been stated in Sec. 3.3 when we said that the qualitative results are consistent with the behavior of flow close to a rotating semi-sphere.

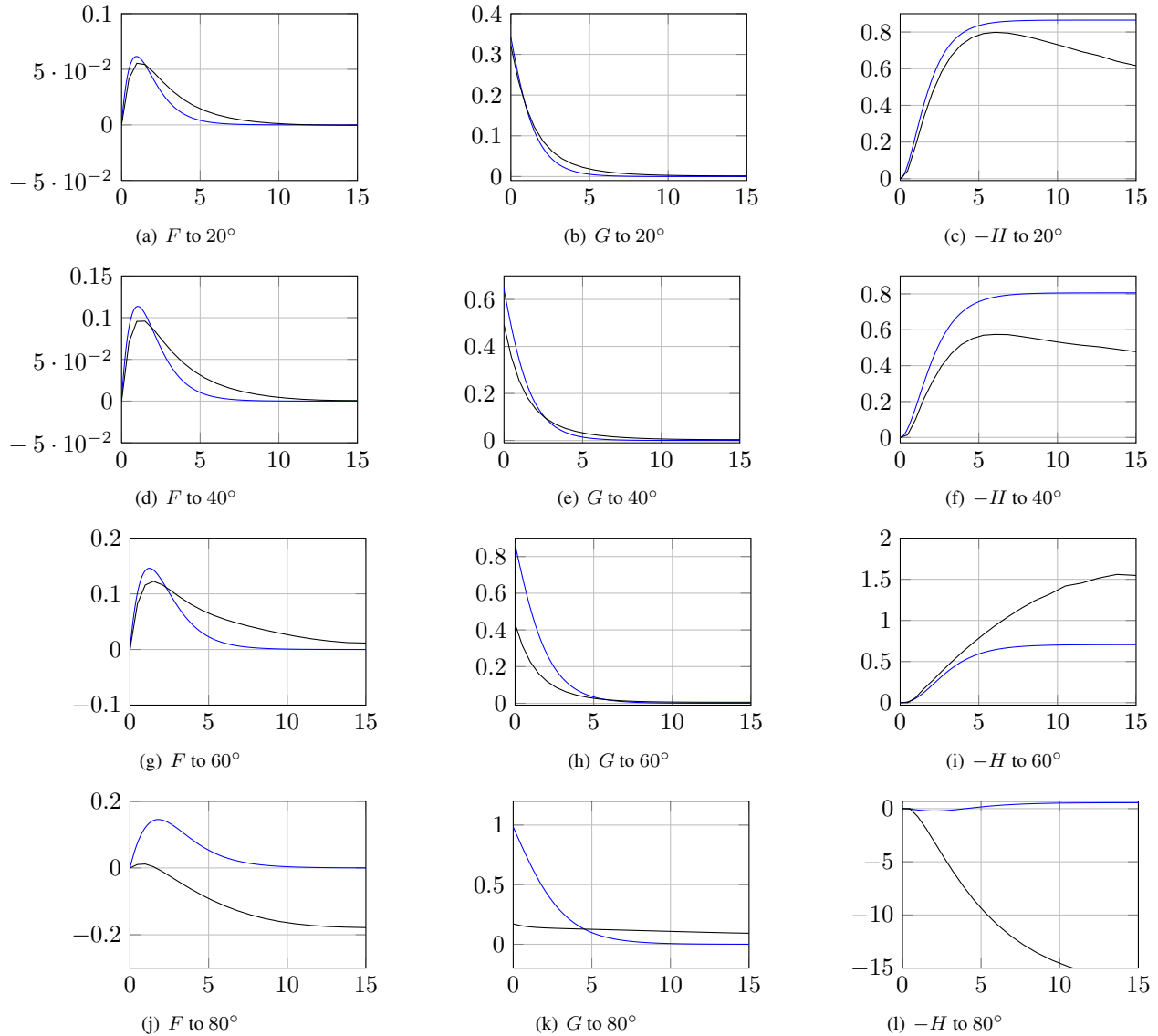


Figure 7. Comparing the profiles F , G and $-H$. Legend: — Analytical solution and — Numerical solution.

The results obtained for the functions F and G to 60° are good, where the function F from a certain radius becomes negative in order to equilibrate the mass balance. And the results for the function H tend towards an asymptotic value as expected from the analytical solution.

For angles greater than 60° the results are not good because it is the region where has a recirculation of the flow.

4. CONCLUSIONS

The results presented are good but they are not sufficient, we need to simulate most cases increasing the radius of the rotating semi-spherical because this determine the Reynolds number involved in the problem. As we want to simulate the flow close the boundary layer we should increase the Reynolds number as a result of the domain of the problem but it requires greater computing cost.

5. ACKNOWLEDGEMENTS

The authors acknowledge financial support from the Brazilian agency CAPES. They also acknowledge the Group of Environmental Studies for Water Reservatories – GESAR/State University of Rio de Janeiro, where most simulations here presented were performed.

6. REFERENCES

- Anjos, G.R., 2007. *Solução do Campo Hidrodinâmico em Células Eletroquímicas pelo Método dos Elementos Finitos*. Dissertação de M.Sc., COPPE/UFRJ, Rio de Janeiro, RJ, Brasil.
- Barcia, O., Godinez, J. and Lamego, L., 1998. “Rotating hemispherical electrode: Accurate expressions for the limiting current and the convective warbug impedance”. *Journal of The Electrochemical Society*, Vol. 145, No. 12, pp. 4189–4195.
- Batchelor, G.K., 2000. *An Introduction to Fluid Dynamics*. Cambridge University Press, Cambridge, 1st edition.
- Bickley, W.G., 1938. *Phil. Mag.*, Vol. 7, No. 25, p. 746.
- Chang, W., Giraldo, F. and Perot, B., 2002. “Analysis of an exact fractional step method”. *Journal of Computational Physics*, , No. 179, pp. 1–17.
- Godinez, J.G.S., 1996. *Eletrodo semi-esférico rotatório: teoria para o estado estacionário*. Tese de D.Sc., COPPE/UFRJ, Rio de Janeiro, RJ, Brasil.
- Howarth, L., 1951. *Phil. Mag.*, Vol. 7, No. 42, p. 1308.
- Hughes, T.J.R., 1987. *The Finite Element Method: Linear Static and Dynamic Finite Element Analysis*. Prentice-Hall, New Jersey, 1st edition.
- Lamb, H., 1932. *Hydrodynamics*. Cambridge University Press, Cambridge.
- Oliveira, G.C.P., 2011. *Estabilidade Hidrodinâmica em Células Eletroquímicas pelo Método de Elementos Finitos*. Dissertação de M.Sc., COPPE/UFRJ, Rio de Janeiro, RJ, Brasil.
- von Kármán, T., 1921. “Über laminare und turbulente reibung”. *ZAMM*, Vol. 1, No. 4, pp. 233–252.

7. RESPONSIBILITY NOTICE

The following text, properly adapted to the number of authors, must be included in the last section of the paper:
The author(s) is (are) the only responsible for the printed material included in this paper.